Jestr

Journal of Engineering Science and Technology Review 7 (4) (2014) 40-45

JOURNAL OF
Engineering Science and Technology Review

www.jestr.org

Mechanics Evolution Characteristics Analysis of Pressure-arch in Fully-mechanized Mining Field

S.R. Wang[1, 3*], N. Li[1], C.L. Li[1, 2] and P. Hagan[4]

[1]*School of Civil Engineering and Mechanics, Yanshan University, Qinhuangdao 066004, China*
[2]*Institute of Urban Construction, Hebei Normal University of Science & Technology, Qinhuangdao 066004, China*
[3]*Opening Laboratory for Deep Mine Construction, Henan Polytechnic University, Jiaozuo 454003, China*
[4]*School of Mining Engineering, University of New South Wales, Sydney, 2052, Australia*

Received 30 March 2014; Accepted 10 September 2014

Abstract

Based on a practical engineering, the three-dimension computational model was built using FLAC^{3D} under the fully-mechanized mining condition. Considering four variation factors, such as the distance of mining advancing, the strength of the surrounding rock, the speed of mining advancing and the dip angle of the coal seam, the mechanics evolution characteristics of the pressure-arch were analyzed. The result showed that for the horizontal seam, the geometric shape of the pressure-arch varied from flat arch to round arch gradually and the height and thickness of the pressure-arch also increased; the maximum principal stress in the skewback also increased with the working face advancing. With the strength of the surrounding rock from soft to hard, the arch thickness reduced, and the arch loading decreased. To improve the mining speed can do some contributions to the stability of the pressure-arch in the mining field. With the increase of dip angle of the seam, the pressure-arch displayed an asymmetric shape, the vault was tilted and moved to the upward direction. At the same time, the thickness of the pressure-arch increased, and the stress concentration in the skewback tended to be further intensified.

Keywords: Pressure-arch, Evolution Characteristics, Mining Field, Fully-mechanized Mining, Numerical Analysis

1. Introduction

With the underground coal mining out, the equilibrium of the original three-dimensional stress of mining field is broken, the stress of the surrounding rock gradually transfers from the mining face to the deep of the rock, and the concentration area of compressive stress will generate within a certain range in the surrounding rock, which forms the pressure-arch in the mining field [1]. The pressure-arch of the mining field is the result of the stress self-regulating. The pressure-arch usually has mechanics properties of the arch structure, which can sustain its loading and transfer the other loads to the foot of the pressure-arch, and this is of great significance to ensure the stability of the surrounding rock of the mining field [2].

Over the past years, many scholars have done the relevant researches on the pressure-arch in the engineering rocks and have made a lot of achievements. For example, W. Hack et al. put forward a pressure-arch hypothesis about the overlying strata movement of the mining field and made a preliminary explanation of the phenomenon of the mining pressure [3]. Z.P. Huang et al. studied the formation mechanism of the natural arch for underground chamber and made a preliminary conclusion [4]. B.A. Poulsen et al. conducted the coal pillar load calculation by pressure arch theory [5]. R. Trueman et al. researched the multiple draw-zone interaction in block caving mines by means of a large physical model [6]. X.D. Liang et al. had defined the pressure-arch of a tunnel, and the inner and outer boundaries of the pressure-arch were determined by the stress analysis, but the determination of outer boundary for the arch body is not clear enough [7]. G.X. Xie et al. had discovered the shell structure of macroscopic stress of the mining field, and studied the influence factors such as mining height and other factors on the mechanical characteristics of the surrounding rock of the fully-mechanized caving face [8]. X.L. Du et al. discussed the stress variation of the mining field with the working face advancing, but the influence factors on the pressure-arch were not considered [9]. Y.M. Geng et al. simulated the variation of the stress arch in the overlying strata after coal mining out by using UDEC [10]. Y.Y. Xu et al. had derived the deflection formulas of the rock slab based on the pressure-arch theory [11], and others studies [12].

In summary, these studies on the geometry parameters and mechanics evolution characteristics of the pressure-arch are still not deep enough, and the discussions are mainly restricted to two-dimensional problem, so an in-depth study on the mechanics evolution characteristics of the three-dimensional pressure-arch in the fully-mechanized mining field is of important theoretical and practical significance.

2. Pressure-arch Geometry Parameters

As shown in Fig. 1, after the coal was mined out, the three-dimensional stress balance of the mining field was broken,

* E-mail address: w_sr88@163.com
ISSN: 1791-2377

then the minimum principal stress at the mining free face became zero, and the stress value gradually increased from the free face to the deep of the surrounding rock until the original stress state. Meanwhile, the maximum principal stress underwent the change from small to the peak value and then decreased to the original stress state too. The pressure-arch formed as a result of the three-dimensional stress self-regulating.

Based on the previous research results, the inner boundary of the pressure-arch are fixed at point A, where is the maximum principal stress (Fig. 1).

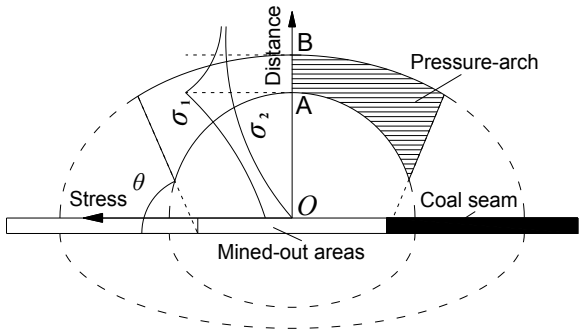

Fig.1. Schematic boundaries of the pressure-arch

In order to determine the outer boundary of the pressure-arch, the variable k is defined as

$$k = \frac{\sigma_1 - \sigma_3}{\sigma_1} \tag{1}$$

Where σ_1 is the maximum principal stress, and σ_3 is the minimum principal stress of the surrounding rock of the mining field. When k is equal to 10 %, the corresponding point B is determined, which is at the outer boundary of the pressure-arch (Fig. 1).

From the two points in the seam floor which also are at both laterals of the mining field as the starting points, two lines are drawn at the rock rupture angle θ and are extended upward respectively, until they meet with the inner and outer boundaries of the pressure-arch, thus the lateral boundaries of pressure-arch are determined as shown in Fig. 1.

The rupture angle θ of the surrounding rock is defined as

$$\theta = 45^0 + \frac{\varphi}{2} \tag{2}$$

Where φ is the inner friction angle of the surrounding rock. The pressure-arch of the surrounding rock is not only in the roof of the mining field but also in both sides and the floor of the mining field. In this paper, the pressure-arch is determined mainly on the top of the mining field as shown in Fig. 1. For the purpose of analysis, the geometry parameters of pressure-arch are shown in Fig. 2.

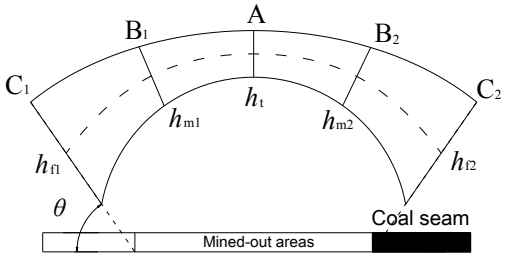

Fig.2. Geometry parameters of the pressure-arch

Taking C_1 line and C_2 line as the skewbacks, where the arch thickness are h_{f1} and h_{f2} and the peak value of the maximum principal stress are P_{f1} and P_{f2}, respectively. And similarly, taking B_1 line and B_2 line as arch waist, where the arch thickness are h_{m1} and h_{m2} and the peak value of the maximum principal stress are P_{m1} and P_{m2}, respectively. The line A represents the vault, where the arch thickness is h_t and the peak value of maximum principal stress is P_t. The dotted line is the central axis of the pressure-arch, and it is called as the pressure-arch curve. As shown in Fig. 2, the smooth pressure-arch curve formed through the median value of the lines between the inner and the outer boundary along the normal direction of the pressure-arch.

3. Three-dimension Computational Model

Taking a practical engineering in a mine as background, after rock group on the roof and floor of the coal seam being generalized, the three-dimension computational model was built using FLAC^{3D} under the fully-mechanized mining condition.

As shown in Fig. 3, the computational model was 240 m long, 240 m wide and 200 m high, and the dimensions of the fully-mechanized mining was 100 m long, 100 m wide and 3.5 m high in the *x*-, *y*-, and *z*-axis, respectively. The fully-mechanized mining was at the depth of 600 m under the ground, and it was in hydrostatic state of stress. There was 600 meter thickness rock above the top of the model, and the vertical load p converted from the rock weight is 15 MPa, where the rock average weight is 25 kN/m^3.

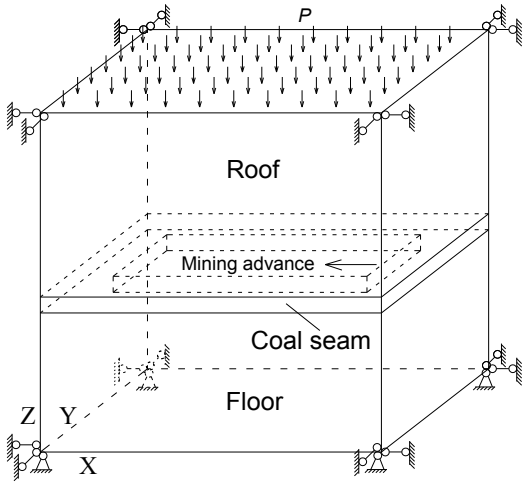

Fig.3. Schematic diagram of the computational model

The horizontal displacement of four lateral boundaries of the model were restricted, the top of the model was applied the vertical load p, and its bottom was fixed. The material of the model was supposed to meet the Mohr-Coulomb strength criterion, and three groups of the physics and mechanics parameters were selected as listed in Table 1.

4. Calculation Results and Discussion

4.1 Distance Variation of the Mining Advancing

Seen from Fig. 4 (a), for the horizontal seam, along the dip of the coal seam, the geometric shape of the pressure-arch

varied from flat arch to round arch gradually with the working face advancing. The height of the pressure-arch increased, and the central axis of the pressure-arch gradually moved to the deep of the surrounding rock from the mining face. Seen from Fig. 4 (b), along the strike of the horizontal coal seam, the pressure-arch varied from the pointed arch to well arched shape, the openings of the pressure-arch increased gradually, and the front foot of the pressure-arch constantly moved forward with working face advancing. Also, the height of the pressure-arch gradually increased.

For the horizontal coal seam, whether along the strike or the dip of the coal seam, the pressure-arch shapes in fully-mechanized mining field were symmetrical, namely $h_{f1} = h_{f2}$, $P_{f1} = P_{f2}$, $h_{m1} = h_{m2}$ and $P_{m1} = P_{m2}$. Therefore, we can take half of the pressure-arch to study the variation characteristics of arch thickness and the maximum principal stress in the arch.

Tab.1 Physical and mechanical parameters of the computational model

Classification	Name	Density (kg/m^3)	Elasticity modulus (GPa)	Poisson ratio	Tensile strength (MPa)	Cohesion (MPa)	Friction angle (°)
Soft rock	Roof	2200	4.5	0.26	1.20	3.5	40
	Coal	1440	3.0	0.28	1.00	3.0	30
	Floor	2300	5.0	0.25	1.50	4.5	42
Medium rock	Roof	2600	20.0	0.25	2.00	8.0	43
	Coal	1440	3.0	0.28	1.00	3.0	30
	Floor	2700	15.0	0.24	3.00	10.0	45
Hard rock	Roof	2600	60.0	0.24	10.00	35.0	48
	Coal	1440	3.0	0.28	1.00	3.0	30
	Floor	2700	80.0	0.23	12.00	40.0	50

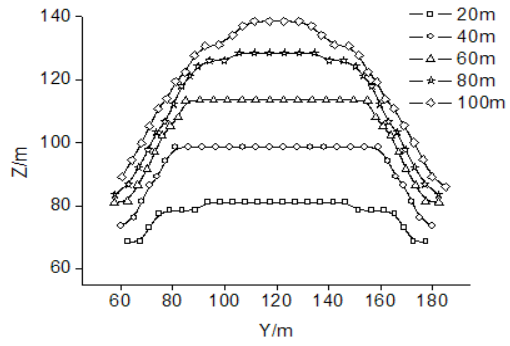

(a) Along dip of coal seam

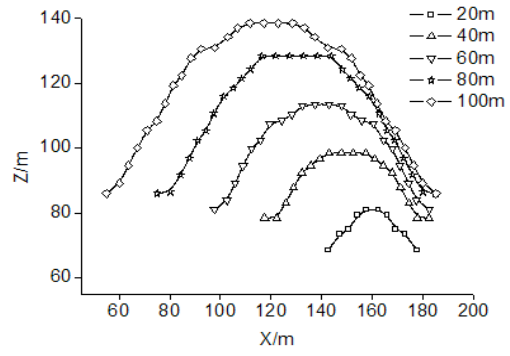

(b) Along strike of coal seam

Fig.4. Shape characteristics of the central axis of the pressure-arch

As shown in Fig. 5, with working face advancing the thickness of skewback, arch waist and vault increased, but the vault thickness would no longer continue to increase until to a certain value, the overall trend was $h_{f1} = h_{f2} > h_{m1} = h_{m2} > h_t$.

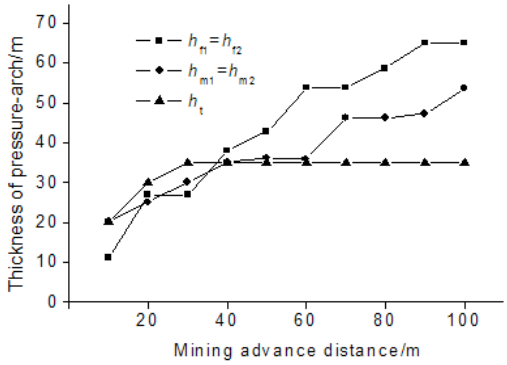

(a) Along dip of coal seam

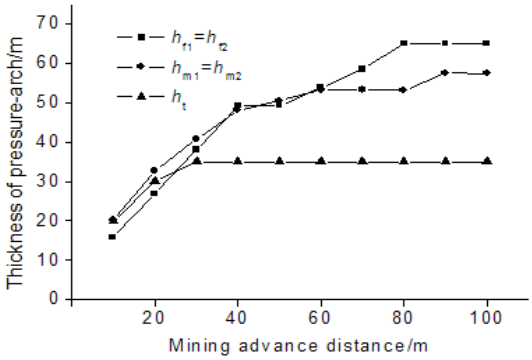

(b) Along strike of coal seam

Fig.5. Thickness variation characteristics of the pressure-arch

Seen from Fig. 6, the maximum principal stress produced in the foot of the pressure-arch. With the working face advancing, the maximum principal stress in the skewback gradually increased, but in other parts the maximum principal stress constantly decreases. The results

showed that the pressure of the skewback increased due to loads passing, so the thickness of the skewback constantly increased with the increase of mining advance distance.

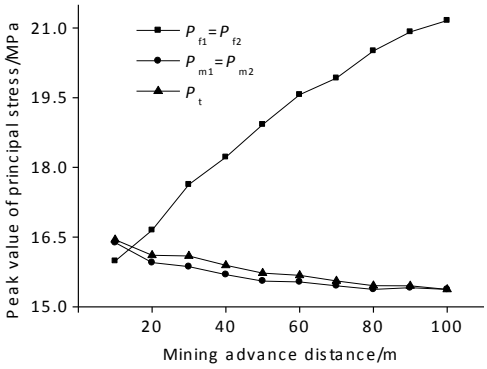

(a) Along dip of coal seam

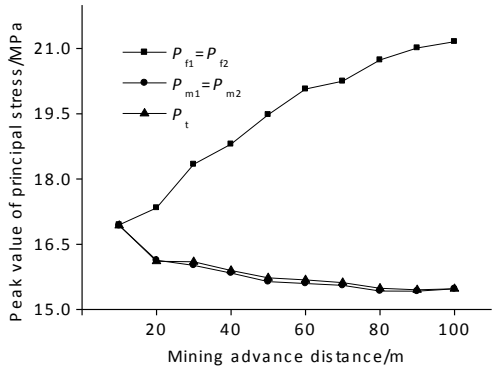

(b) Along strike of coal seam

Fig.6. Peak value of principal stress variation of the pressure-arch

4.2 Rock Strength Variation of the Mining Field

Seen from Fig. 7, with the strength of the surrounding rock from soft to hard, along the dip of the seam, the pressure-arch shape changed from flat-top arch to round arch, and the height of the arch-pressure was getting away from the mining face. Along the strike of the seam, the pressure-arch shape changed from the flat-top arch to the pointed arch gradually.

Overall, with the strength of the surrounding rock from soft to hard, except that the vault thickness had a slight increase, the thickness of the other parts of the pressure-arch decreased (See Fig. 8). Meanwhile, as shown in Fig.9, the peak value of the maximum principal stress in the arch foot demonstrated a significant decreasing trend. Thus, the higher the rock strength was, the more easily the pressure-arch formed. The arch thickness reducing showed that the arch loading was reducing, and the decrease of peak value of the maximum principal stress in the pressure-arch showed that the mining field was more stability.

4.3 Velocity Variation of the Mining Advancing

Assumed three mining speed was 5 m/week, 10 m/week and 20 m/week, the calculation results were shown in Fig. 10. Seen from the Fig. 10, the slower the mining speed was, the more obvious stress the concentration phenomenon of the surrounding rock was. Therefore, to improve the mining speed can significantly reduce the stress concentration in the surrounding rock in front of the working face, and also can do some contributions to the stability of the pressure-arch in the mining field.

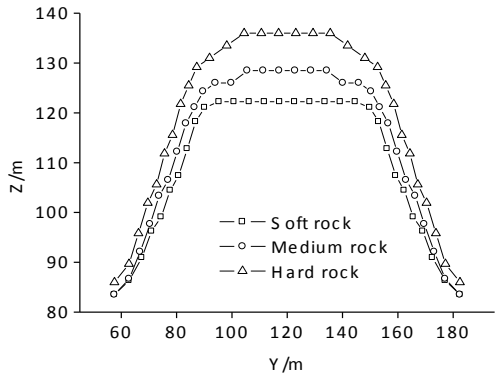

(a) Along dip of coal seam

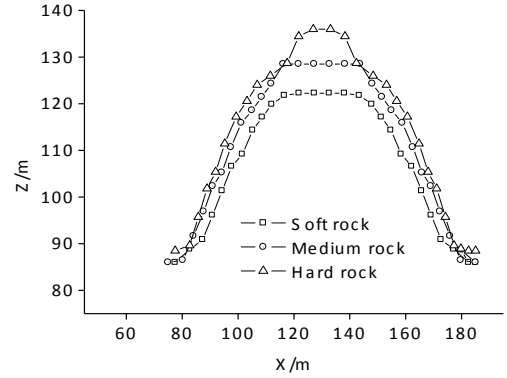

(b) Along strike of coal seam

Fig.7. Shape characteristics of the central axis of the pressure-arch

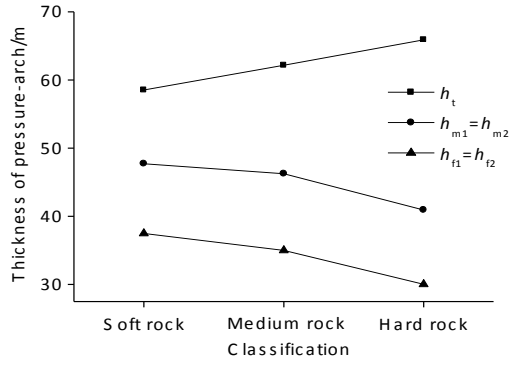

(a) Along dip of coal seam

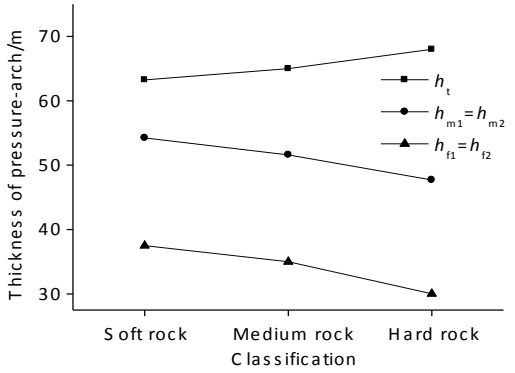

(b) Along strike of coal seam

Fig.8. Thickness variation characteristics of the pressure-arch

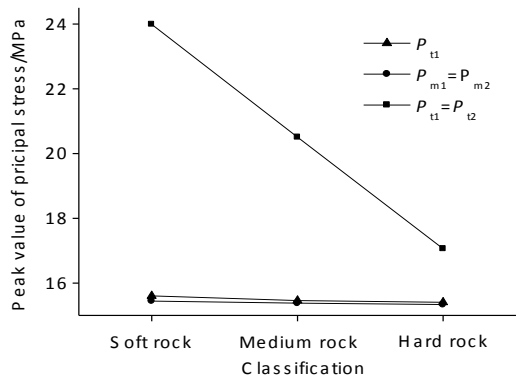

(a) Along dip of coal seam

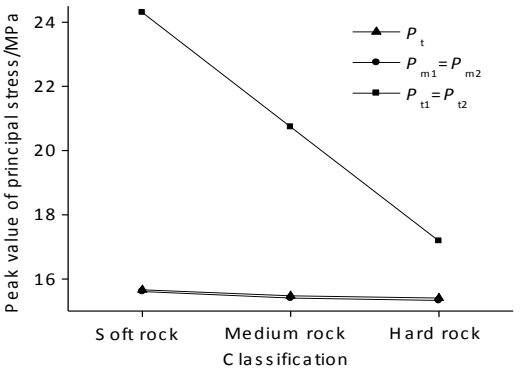

(b) Along strike of coal seam

Fig.9. Peak value of principal stress variation of the pressure-arch

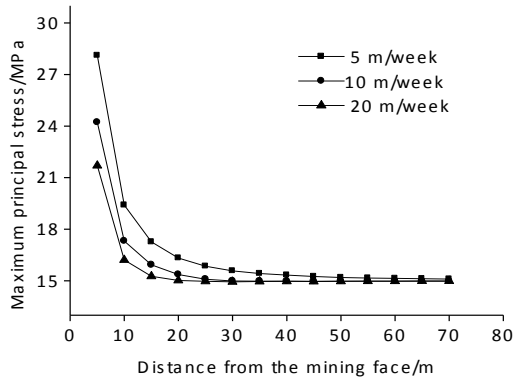

Fig.10. Maximum stress variation with mining speed

4.4 Dip Angle Variation of the Coal Seam

Fig. 11 demonstrates the geometry parameters of the pressure-arch with dip α of the coal seam.

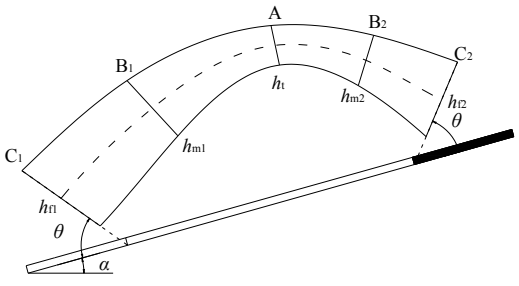

Fig.11. Asymmetric shape of pressure-arch

As shown in Figs. 12, 13 and 14, with the dip angle of the coal seam changing from 0 º, 10 º, 20 º to 30 º along the strike of the seam, the pressure-arch was symmetrical. But along the dip of the seam, the pressure-arch displayed an asymmetric shape, and the vault was tilted and moved to the upward direction. The greater the dip angle was, the more apparent the inclination of the pressure-arch was. The arch thickness and peak stress is not asymmetric, that is $h_{f1} \neq h_{f2}$, $P_{f1} \neq P_{f2}$, $h_{m1} \neq h_{m2}$, $P_{m1} \neq P_{m2}$.

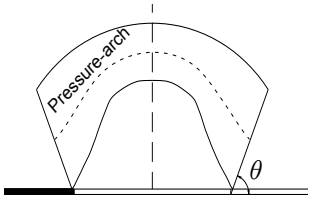

(a) 0°

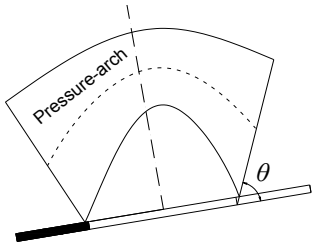

(b) 10°

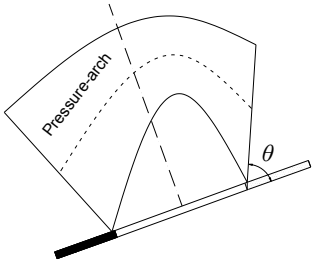

(c) 20°

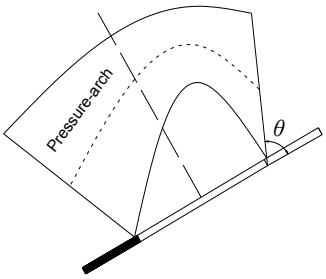

(d) 30°

Fig.12. Pressure-arch shape characteristics with different dips

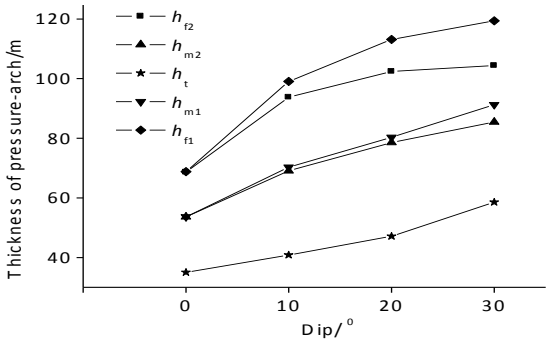

(a) Along dip of coal seam

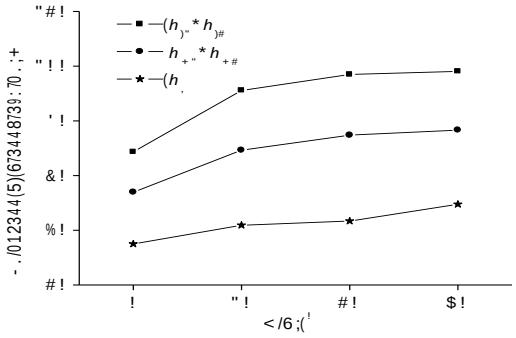

(b) Along strike of coal seam

Fig.13. Thickness variation of the pressure-arch with different dips

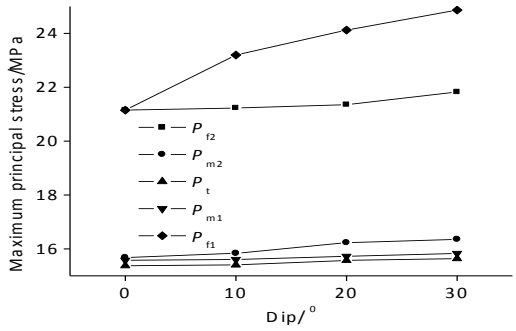

(a) Along dip of coal seam

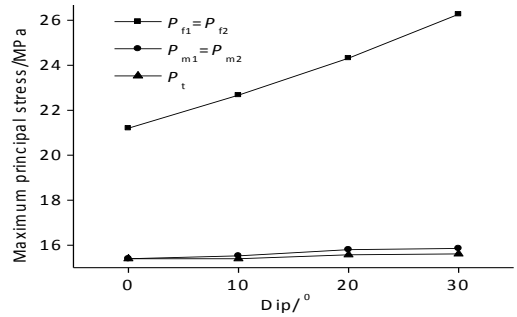

(b) Along strike of coal seam

Fig.14. Peak value of principal stress variation with different dips

Seen from Figs. 12 and 13, with the dip angle of the coal seam increased, the arch thickness and the maximum principal stress also increased, and the increasing trend of the thickness was $h_{f1} > h_{f2} > h_{m1} > h_{m2} > h_t$ in general. Meanwhile, the skewback located in the low position of the pressure-arch would bear more loading, and the stress concentration tended to be further intensified (Fig. 14).

5. Conclusion

For the horizontal seam, with the working face advancing, the geometric shape of the pressure-arch varied from flat arch to round arch gradually in the fully-mechanized mining field. The height of the pressure-arch increased, and the thickness of skewback, arch waist and vault also increased.

With the strength increase of the surrounding rock from soft to hard rock, the thickness and the loading of pressure-arch decreased. To improve the mining speed can significantly reduce the stress concentration in the surrounding rock in front of the working face, and that can do some contributions to the stability of the pressure-arch in the mining field.

With the increase of dip angle of the coal seam, along the dip of the seam, the pressure-arch displayed an asymmetric shape, and the vault was tilted and moved to the upward direction. Meanwhile, the stress concentration tended to be further intensified, and the skewback located in the low position of the pressure-arch would bear more load than the other one.

Acknowledgments

This work was financially supported by the National Natural Science Foundation of China (51474188; 51074140; 51310105020), the Natural Science Foundation of Hebei Province of China (E2014203012) and Program for Taihang Scholars, all these are gratefully acknowledged.

References

[1]. Wu Y.-P., Wang H.-W. and Xie P.-S., "Analysis of surrounding rock macro-stress arch-shell of long-wall face in steeply dipping seam mining", *Journal of China Coal Society*, 37 (4), 2012, pp. 559-564. (in Chinese)

[2]. Wang S.-R., Wang H. and Hu B.-W., "Analysis of catastrophe evolution characteristics of the stratified rock roof in shallow mined-out Areas", Disaster Advances, 6 (S_1), 2013, pp. 59-64.

[3]. Mark B., "Analysis of ground support methods at the kristinederg mine in Sweden", *Proc. 16th Canadian Rock Mechanics Symposium and the International symposium on Rock support*, Canada, Rotterdam, 1992, pp. 499-506.

[4]. Huang Z.-P., Broch E. and Lu M., "Cavern roof stability-mechanism of arching and stabilization by rock bolting", *Tunnelling and Underground Space Technology*, 17 (3), 2002, pp. 249-261.

[5]. Poulsen B.-A., "Coal pillar load calculation by pressure arch theory and near field extraction ratio", *International Journal of Rock Mechanics and Mining Sciences,* 47 (7), 2010, pp. 1158-1165. (in Chinese)

[6]. Trueman R., Castro R. and Halim A., "Study of multiple draw-zone interaction in block caving mines by means of a large 3D physical model", *International Journal of Rock Mechanics and Mining Sciences,* 45 (7), 2008, pp. 1044-1051.

[7]. Liang X.-D., Zhao J. and Song H.-W., "Experimental and numerical analysis on the arching action from stress adjusting in surrounding rocks", *Journal of Engineering Geology*, 20 (1), 2012, pp. 96-102. (in Chinese)

[8]. Xie G.-X., "Influence of mining thickness on mechanical characteristics of working face and surrounding rock stress shell", *Journal of China Coal Society*, 31 (1), 2006, pp. 6-10. (in Chinese)

[9]. Du X.-L. Song H.-W. and Chen J., "Numerical simulation of the evolution of the pressure-arch during coal mining", Journal of *China University of Mining & Technology*, 40 (6), 2011, pp. 863-867. (in Chinese)

[10]. Geng Y.-M., "Study on evolution law of stress arch of overlying strata in mines", *Journal of Shandong University of Science and Technology (Natural Science)*, 28 (4), 2009, pp. 43-47. (in Chinese)

[11]. Xu Y.-Y., Yu G.-M., Li C.-J. Xu J.-F. Zhang M.-P. and Meng D., "Study on the laminated board - unloading arch model of the Mining overburden", *Mining Safety & Environmental Protection*, 33 (3), 2006, pp. 7-10.

[12]. Xie Z., Luan T. and He N., "Numerical simulation of air leakage in goaf of fully mechanized face with high dip and hard roof", *Computer Modelling and New Technologies*,17 (2), 2013, pp. 36-43.